Single Phase Turbulent Flow Regime Characterization Using Image Processing Techniques

by

Yong Hong Yaw

15939

Dissertation submitted in partial fulfillment of

The requirements for the

Bachelor of Engineering (Hons.)

Mechanical Engineering

January 2016

Universiti Teknologi PETRONAS
Bandar Seri Iskandar
31750 Tronoh
Perak Darul Ridzuan

CERTIFICATION OF APPROVAL

Single Phase Turbulent Flow Regime Characterization Using Image Processing Method

by

Yong Hong Yaw

15939

A project dissertation submitted to the

Mechanical Engineering Programme

Universiti Teknologi PETRONAS

in partial fulfillment of the requirements for the

Bachelor of Engineering (Hons.)

Mechanical Engineering

Approved by,

____

(Dr. Mark Ovinis)

UNIVERSITI TEKNOLOGI PETRONAS

TRONOH, PERAK

January 2016

CERTIFICATION OF ORIGINALITY

This is to certify that I am responsible for the work submitted in this project, that the original work is my own except as specified in the references and acknowledgements, and that the original work contained herein have not been undertaken or done by unspecified sources or persons.

____

YONG HONG YAW

ABSTRACT

Optical techniques are useful for non- contacting flow measurements such as high pressure and high temperature situations. Certain optical flow measurement technique works well only in turbulent flow regime. Hence, in order to improve the optical flow measurement technique, there is a need to characterize the single phase turbulent flow regime using image processing technique. This will allow the optical flow measurement technique to be applied at the turbulent flow regime, increasing its accuracy. Crone et. al. stated in his Optical Particle Velocimetry (OPV) work that OPV works best in turbulent flow regime. It cannot be applied to transitional flow regime. Image processing techniques was applied on 50 frames of Crone et. al.'s single phase flow images to characterize the single phase turbulent flow regime. Experimental results developed by Crone et. al. was used as the theoretical data to validate the accuracy of the techniques. Results shown that thresholding and features matching techniques were able to characterize the single phase turbulent flow regime. The percentage error of the techniques is approximately 5% and 60% respectively. The error may be caused by limitation of the image processing technique itself and the inaccuracy of the training images used by feature matching technique. For feature matching technique, an additional trial was performed on accurate training images and the error percentage was reduced to 20%. Textural filters technique was unable to detect the turbulent flow regime. This maybe caused by the textural properties of the flow image is the same within a flow. Various textural filters were applied on the image, yet all yield no results. More test images are needed to improve and validate the accuracy of the techniques. Future recommendations will be suggesting to perform work on study of the optical properties of various flow regimes, develop flow regime characterization technique that are able to characterize all three flow regimes and perform study of the technique on different types of single phase flow.

ACKNOWLEDGEMENT

This 8 months of informative final year project cannot be made possible without the sincere contribution of the following parties.

Hereby, I would like to express my upmost gratitude to my university, Universiti Teknologi PETRONAS especially the mechanical engineering department for giving me this golden opportunity to conduct my final year project as per the university's requirement, giving me a taste of doing research work. My heartfelt appreciation goes to my supervisor, Dr Mark Ovinis for his constant guidance and support throughout this journey; my graduate assistant Mr. Osman Ano and Mr. Lu Fan for their kind assistance and the knowledge they shared; my internal examiner, Assoc. Prof. Dr. Fakhruldin bin Mohd. Hassim and external examiner, Mr. Muhammad Izzat for your willingness to spare your precious time to evaluate and provide constructive recommendation to my project.

Not to forget my ever helpful friends and course mates for always being there to provide me the motivation and moral support. A great thank you I would like to mention to my family members especially my parents for always having faith in me, being there for me, constantly providing me with the moral and financial support and provide me a chance for higher education. They had been very forgiving and constantly supportive on the journey that I am currently pursuing.

Without all your sincere support and assistance, I will not be able to complete my final year project with flying colours.

Thank you.

Table of Contents

LIST OF FIGURES

LIST OF TABLE

CHAPTER 1

INTRODUCTION

1.1 Background

In the year of 2010, a tragedy occurred in the Gulf of Mexico, off Louisiana Coast. A semi- submersible drilling rig owned by British Petroleum (BP) drilling at Mocando field had experienced a well blow out. [1] Barrels and barrels of hydrocarbon spilled out of the oil field uncontrollably. In order to access the damage done by the oil spill to the environment, the National Incidence Command (NIC) requested industrial experts to estimate the volume of hydrocarbon that spilled out from the well. Various flow measurement technique was opt for. Airborne Visible/ Infrared Imaging Spectrometer and optical flow measurements were some of the technique used. Mcnutt et. al. [1] stated that intrusive measurement techniques will fail due to icing caused by hydrates. That time, there was no proven methods for directly measuring the hydrocarbon discharge at the given temperature and pressure. Optical flow measurements such as particle image velocimetry (PIV), optical plume velocimetry (OPV) and laser Doppler technique used by oceanographers to quantify flow rate from deep sea hydrothermal vent was used to perform the estimate. Reservoir modelling was deployed as well to investigate the amount of hydrocarbon that was released from the reservoir.

PIV analysis software tried to measure the velocity of the visible features (vortices, eddies, white particles that are presumed to be hydrates). Feature- tracking velocimetry (FTV) was used to visually detect the displacement of the recognizable features. The volumetric flow rate was then calculated by multiplying the measured jet velocity with the cross- sectional area of the jet with corrections for gas- to- oil ratio (GOR). Mcnutt et. al. [1] states that PIV analyses performed by experts produced flow rate estimates of about one- half the magnitude of the estimates of other methods, even using the same video observation. Crone & Tolstoy [2] stated in their work prior to Deep Water Horizon accident that PIV would underestimate flow rates by about a factor of 2 when applied to turbulent buoyant jets. After a series of study on the flow rate estimates the Flow Rate Technical Group (FRTG) had concluded the flow rate out of the well head is between 50,000 to 70,000 barrels per day. Apart from PIV, the other techniques all conform to the estimates provided by FRTG on the estimated flow rate of hydrocarbon escaping the well.

The incident above is an example of application of optical flow measurement technique. Optical flow measurement techniques can be used in situations where flow conditions are high in pressure and temperature. Inserting a probe/ sensor into such flow may damage the probe/ sensor. Examples of established flow measurement techniques are such as laser Doppler technique, PIV and OPV. [3-6] Crone et. al.'s work on OPV was able to yield an accurate flow estimates for the Deep Water Horizon Oilspill incident. The technique is able to estimate the flow rate of a fluid flow optically using cross correlation technique.

1.2 Problem Statement

Optical flow measurement techniques such as OPV and PIV have its limitation. For OPV as per say, OPV works best at turbulent flow regime. It is not reliable in transitional flow regime. [6] PIV on the other hand, when it was applied on turbulent buoyant jets, it may yield a lower result. [2] Thus, this provides the motivation to develop a turbulent flow regime characterization technique using image processing technique. With the knowledge of the single phase turbulent flow regime, the accuracy of the optical flow measurement technique should be increased. Turbulent flow is flow with chaotic properties. It is distinct in terms of optical appearance when compared to the other 2 flow regimes. (laminar and transitional) These differences are in terms of gray level, entropy and energy. Besides, features such as vortices and saddles can be used to distinguish the flow regime. Figure 1.1. & 1.2 shows example of vortices that are able to be used as features to classify single phase turbulent flow regime. These features and differences presence in a single phase turbulent flow enable us to track, classify and distinguish single phase turbulent flow regimes with other single phase flow regimes.

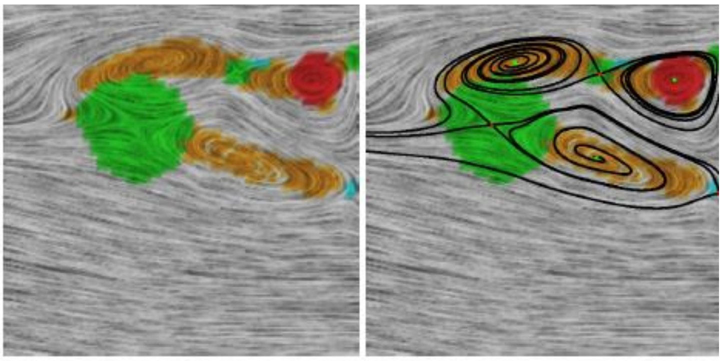

FIGURE 1.1: Left: Image of vortices generated by an ICE train. Right: Previous image added with topology for improved observation. [7]

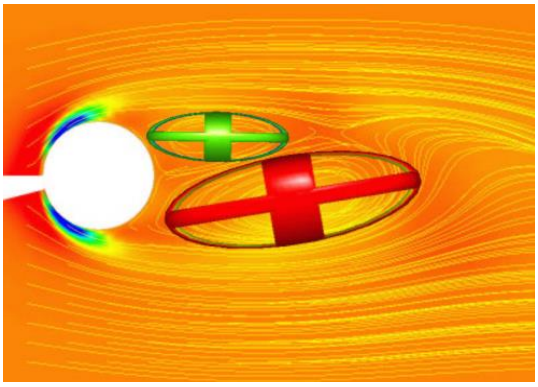

FIGURE 1.2: Image of vortices behind a tapered cylinder. [10]

1.3 Objectives

The objectives of this final year project are as follows:

1. To develop single phase flow regime characterization algorithm using image processing technique

1.4 Scope of Study

The scope of study for this final year project focuses on the following aspects:

1. Single phase fluid flow
2. Turbulent flow regime
3. Image processing techniques

CHAPTER 2

LITERATURE REVIEW

This project uses several image processing techniques to characterize the single phase turbulent flow regime. Hence, application of image processing techniques will be discussed in this topic.

2.1 Image Processing Techniques

2.1.1 Thresholding

Tobias [11] stated in his work on image segmentation by histogram thresholding using fuzzy sets that image segmentation process is used to separate the area of interest and the background into non-overlapping sets. When thresholding method is applied to the image, pixels whose gray level exceed the critical value will be assigned to one set, the rest will be assigned to the other set. Tobias mentioned that the optimum threshold value using histogram thresholding technique must be located in the deep valley between the two peaks of histogram. [11] Tobias stated that histogram thresholding technique works well when the image- gray level histogram is bi-modal/ double peak. The technique performs poorly or even fail when the image is corrupted with noise or irregularly illuminated. To find the reliable threshold limit, criterion for splitting image histogram should be use. Ridler and Calvard stated that the success of the thresholding technique relies on the object that is desired to be extracted. The optimum threshold value is difficult to determine. If the value is too high, there will be a loss of information and if value is too low, there will be a rise to objectionable background clutter. [12]

Weszaka et. al. [13] agrees with Tobias's work. They stated that the common method of deriving the threshold value of a picture is by examining the gray level histogram. The presence of two peaks indicates the existence of two distinct brightness region in one image. One corresponds to the image of interest, the other one is the surrounding. The reasonable way to choose the threshold value is by choosing the gray level midway between the two peak. Otsu [14] stated in his work that when facing difficulties to perform thresholding due to no traceable valley in the gray level histogram, one shall perform some valley sharpening technique. These techniques can be either Lapacian, gradient or difference histogram method, select the threshold at the gray level with the maximum amount of difference. These methods then modify the histogram using the information of the neighboring pixels to make it useful for thresholding.

1.1.2 Feature Matching

Ebling et. al. [9] produced a work on segmenting vector fields using template matching. The work used template matching approach as pattern matching approach has already been proven useful for detection and quantification of features in flow fields. [10] The features of interest such as vortex, saddle, sink, shear, the strength, the size and the scale at which they appear are determined prior before segmentation process. Post et. al. [11] stated in his work that features used in features extraction can be as of any objects, structures or regions that is in relevance to a particular research. For fluid dynamics, vortexes, shock waves, boundary layers and recirculation zones can be a feature for feature extractions.

1.1.3 Textural filter

Saviee and Rezai Rad [15] produced a work on sidescan sonar images textural segmentation using Gabor filters banks and active contours without edges. The original sonar image will be passed through a Gabor filters bank. Filters in the bank are of same central radial frequency and different orientations. A new filtered image with a significant component of the original one will be produced. The filtered image is smother when compared to the original image and lastly, Chan and Vese multi-channel active contours method are applied on the filtered image to detect the boundaries of the regions with different texture.

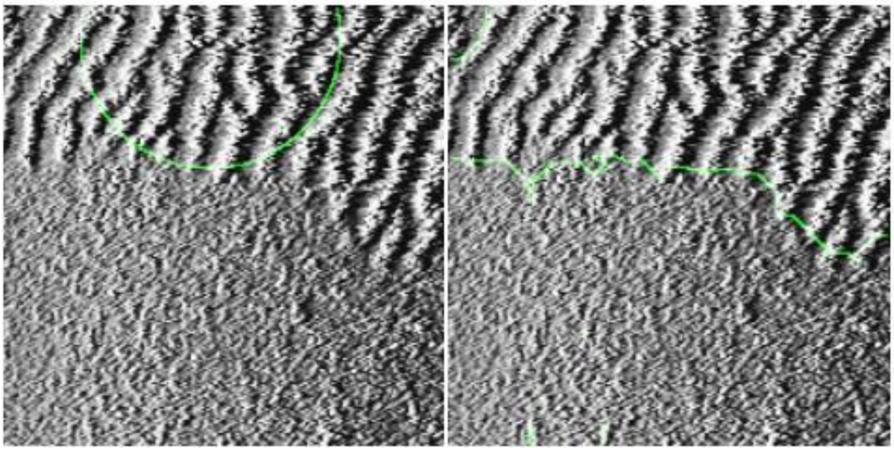

FIGURE 2.1 Detection boundary of two different textural regions in a side scan sonar image with an interior contour [15]

Sindhuja and Sadasivan [16] produced a work on unsupervised textural segmentation of SonoElastographic breast images. The textural features were used by Sindhuja and Sadasivan to differentiate benign and malign breast cells. They also stated that most of the textural segmentation method available incorporate spatial frequency and local edge information. This result in a more computationally demanding technique. [16] Textural segmentation is commonly used in classification problems mainly for diagnostic purposes where the region of interest is delineated manually. [17,18]

CHAPTER 3

METHODOLOGY

3.1 Project Activities

This project will be using the experimental data from Crone et. al. ‘s work [6] as the basis of the project. Crone’s image as shown in figure 3.1 will be used to validate the results developed.

FIGURE 3.1 Experimental images developed by Crone et. al. [6]

Images obtained from a single phase fluid flow will be preprocessed to define the area of interest. The 8 bit, 332 x 248 resolution, grey scale image of the flow will be cropped the resolution of 305 x 371 to remove the unwanted area. A preprocessed image is as shown in figure 3.2. The image processing technique that will be used are thresholding, features tracking, and textural filters. The flow regimes are characterized by determining the characteristic length for the fluid to turn turbulent from the nozzle. A total of 50 frames were obtained from Crone et. al.’s video to determine the accuracy of the techniques. The textural filter that will be used in the project is entropy filter with entropy thresholding.

FIGURE 3.2 Preprocessed image

According to Spurk and Aksel [19], the critical Reynolds number for the fluid to become turbulent can be as high as 40,000 especially in situations free of disturbance. For flow which is highly disturbed the critical Reynold's number drops to 2,300. The recommended valid measurement for critical Reynold's number given the conditions found in technical application will be 2,300. This is the value that will be used to determine the characteristic length. For Crone et. al.'s experiment, the jet fluid used is tap water added with approximately 0.5 wt% Sodium Chloride to provide buoyancy flux. The main tank is filled up with tap water. [6] Table 3.1 shows the different density of the materials used in Crone et. al.'s experiment. The experiment conducted by Crone et. al. is at room temperature, approximately 23 ˚C. The kinematic viscosity for water at 23 ˚C is 3.4049 x 10^{-6} m^2/s [20].

TABLE 3.1 Density of different materials used.

Materials	**Density (kg/m^3)**
Sodium Chloride, NaCl	2600.00
Water, H_2O	999.00
Water with 0.5 wt% of Sodium Chloride, NaCl	999.21

Equation 3.1 is the equation used to calculate Reynold's number, where v is the flow velocity, L is the characteristic length and ν is the kinematic viscosity.

$$Re = \frac{vL}{\nu} \quad \text{Eqn 3.1}$$

3.2 Process Flow Chart

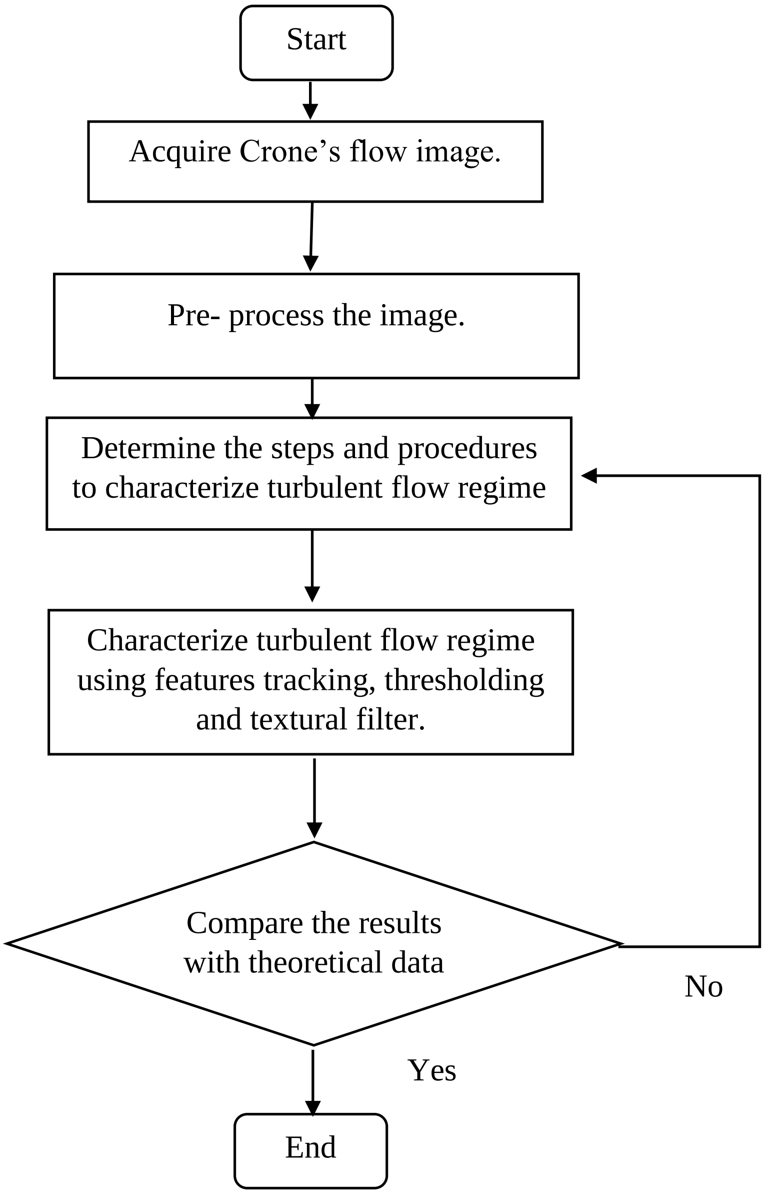

FIGURE 3.2 Flow chart of the project activities.

3.3 Image Processing Technique Procedure

3.3.1 Thresholding

Steps for thresholding algorithm is as follow:

1) Read the single phase flow image
2) Convert RGB image into gray scale and crop the region of interest.
3) Define the thresholding limit. The threshold limit should be in between the double peak of the image's histogram.
4) Threshold the image to identify the turbulent flow regime.
5) Repeat step 3 and step 4 by varying the threshold limit with the value of 0.1.
6) Validate the results by comparing with the theoretical results.
7) Repeat step 1 – 8 for the remaining 49 frames

3.3.2 Point Feature Matching

Steps for point feature matching algorithm is as follow:

1) Read both the images (Single phase flow and single phase turbulent flow regime)
2) Convert RGB image into gray scale and crop the region of interest.
3) Detect the 100 strongest feature points in the single phase turbulent flow image and detect the 500 strongest feature points in the single phase flow image.
4) Extract the feature point descriptors from both the images.
5) Match the feature point descriptors for both the images.
6) Locate the single phase turbulent flow using the putative matches.
7) Display the detected region.
8) Validate the results by comparing with the theoretical results.
9) Repeat step 1 – 8 for the remaining 49 frames

3.3.3 Textural Filter

Steps for textural filter segmentation algorithm is as follow:

1) Read single phase flow image.
2) Convert RGB image into gray scale and crop the region of interest.
3) Create rough textural mask for the turbulent texture using entropy filter. Entropy filter returns an array where each output pixel contains the entropy value of the 9 x 9 neighborhood around the corresponding pixel in the image.
4) Threshold the rescaled image to segment the features. A threshold value of 0.4 is selected because it is roughly the intensity value of pixels along the boundary between the textures.
5) Use rough mask to segment the turbulent texture
6) Display the detected region.
7) Validate the results by comparing with the theoretical results.
8) Repeat step 1 – 8 for the remaining 49 frames

3.4 Project Key Milestones

The key milestones for this project will be

i) Data acquisition by obtaining images for Crone's experimental flow. [6]
ii) Identify the turbulent flow regime.
iii) Compare the accuracy of the three image processing algorithm.

3.5 Gantt Chart

TABLE 3.2 Gantt chart for FYP I & II

FYP I (September 2015 semester)

Project activities/ Weeks	**1**	**2**	**3**	**4**	**5**	**6**	**7**	**8**	**9**	**10**	**11**	**12**	**13**	**14**
Literature review and research work														
Project planning														
Selecting the image processing technique														
Hands on work on MATLAB with trial data														
Image acquisition from Crone's experimental flow														**X**

FYP II (January 2016 semester)

Project activities/ Weeks	**1**	**2**	**3**	**4**	**5**	**6**	**7**	**8**	**9**	**10**	**11**	**12**	**13**	**14**
Theoretical calculation														
Classifying the turbulent flow regime							**X**							
2^{nd} trial with different images														
Algorithm validation											**X**			

X - Key milestones

CHAPTER 4

RESULTS AND DISCUSSIONS

4.1 Theoretical Results

The following is the theoretical results of the characteristic length for the fluid to turn turbulent using Crone et. al.'s experimental images [6]. The theoretical results are calculated using Reynold equation. Since the density of the mixture is close to the density of water and 99.5% wt of the solution is tap water. It is safe to say that the parameters used for calculating the theoretical characteristic length can be taken as water. The mean nozzle velocity used was 0.27 m/s. Characteristic length is as the following

$$Re = \frac{vL}{\nu}$$

2,300 = 0.27 m/s (L)/ (3.4049 * 10^-6)

L = 0.029 m

4.2 Image Processing Technique Results

4.2.1 Image segmentation using thresholding

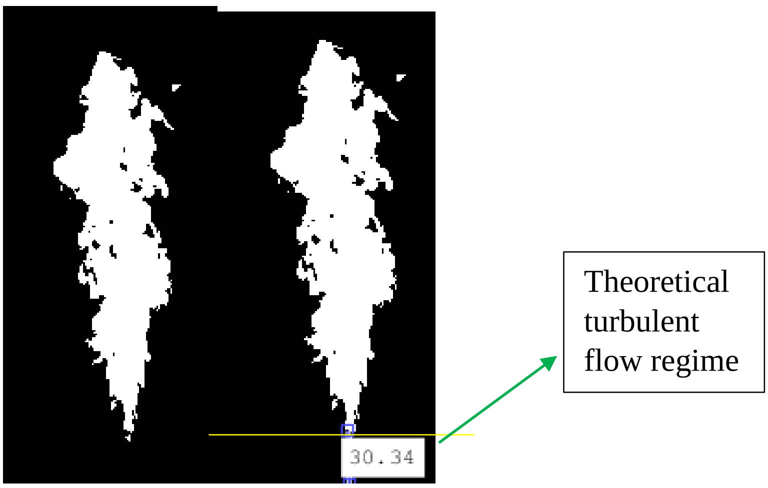

FIGURE 4.1 Left: Image processed using threshold value of 0.4. Right: The experimental distance of turbulent region from nozzle (in pixels).

Based on figure 4.1, we can see that the chaotic properties of single phase turbulent flow can be distinctly differentiated from the other single phase flow regimes. The best observation of single phase turbulent flow is when the thresholding limit is set at 0.4. Figure 4.2 shows the histogram of the original pre-processed image. The histograms show a single peak histogram with the peak leaned towards the left side. With a threshold value of 0.4, pixel with grey level higher than 102 will be converted into black and pixels with grey level lower than 102 will be converted into white. The chaotic properties of single phase turbulent flow produce an intensity lower than 102 when compared to single phase laminar region which is smooth and clam. This feature enables the thresholding algorithm to differentiate the single phase turbulent region and other regions. As per Crone et. al.'s work, 1 m in the image contains 868 pixels. [6] The actual characteristic length will be calculated by multiplying the characteristic length in pixel with 1.1655 * 10 ^ -3 m.

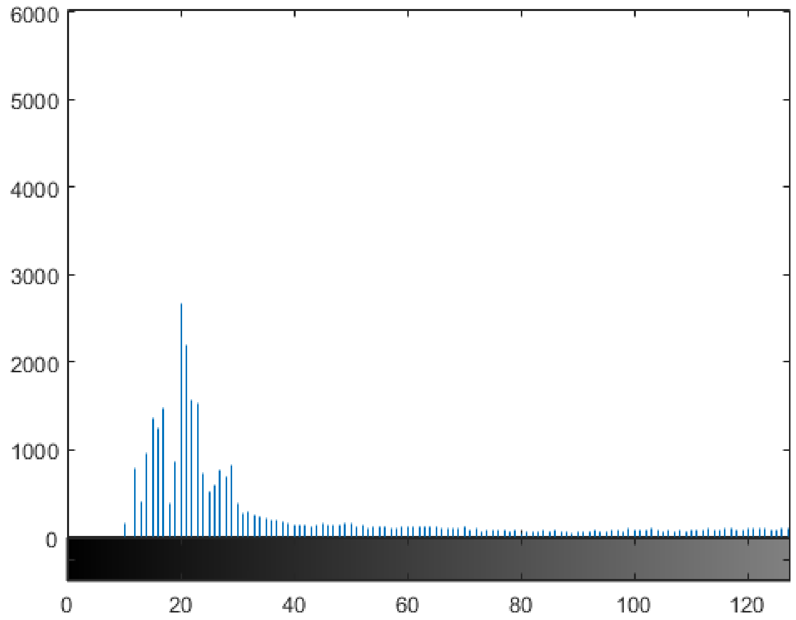

FIGURE 4.2 Histogram of the pre-processed image.

4.2.2 Image segmentation using feature tracking

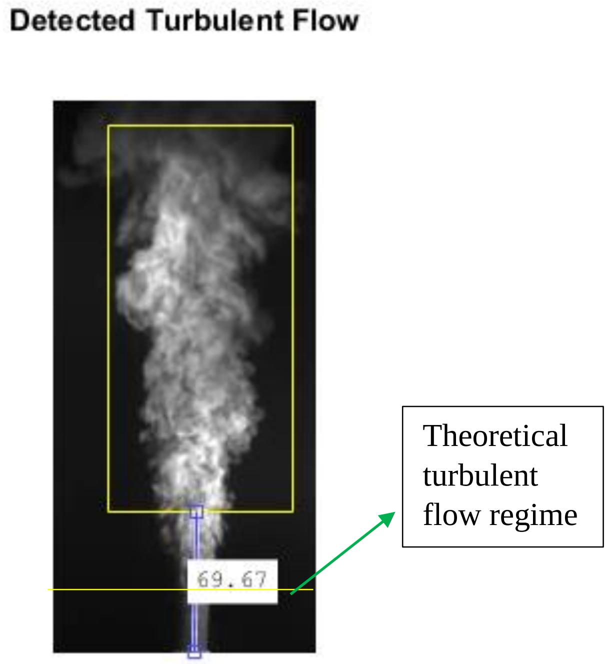

FIGURE 4.3 Detected single phase turbulent flow region using feature tracking.

The figure above shows us the visual observation of single phase turbulent flow region identified using feature tracking algorithm. The box in the image is the detected single phase turbulent flow regime. The chaotic properties of single phase turbulent region are distinct when compared with single phase laminar region. The feature tracking algorithm tracks the strong points of a predefined single phase turbulent flow and it will match it with the experimental image. It is believed that the strong points in single phase turbulent flow regime are the vortices and ripples. These features allow the algorithm to trace it in flow image.

4.2.3 Image segmentation using textural filter

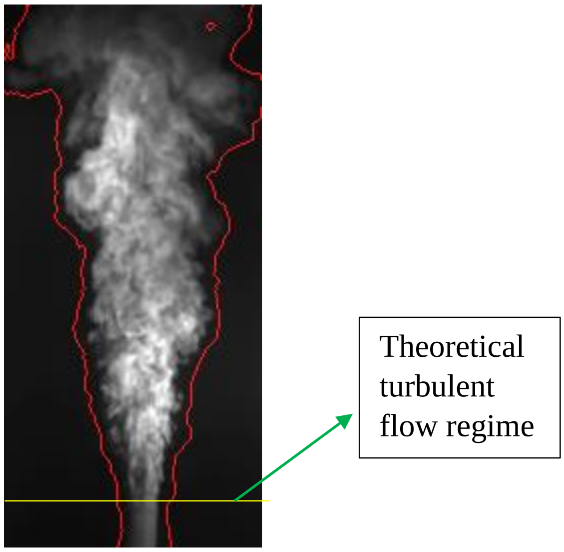

FIGURE 4.4 Detected single phase turbulent flow region using textural filter.

The figure above shows us the visual observation of single phase turbulent flow regime identified using textural filter. The red line determines the segmented region in terms of textural properties. The technique is unable to differentiate the turbulent flow regime with other flow regime. The red line in the image defines the region characterized by the technique.

4.2 Overall Result and Discussion

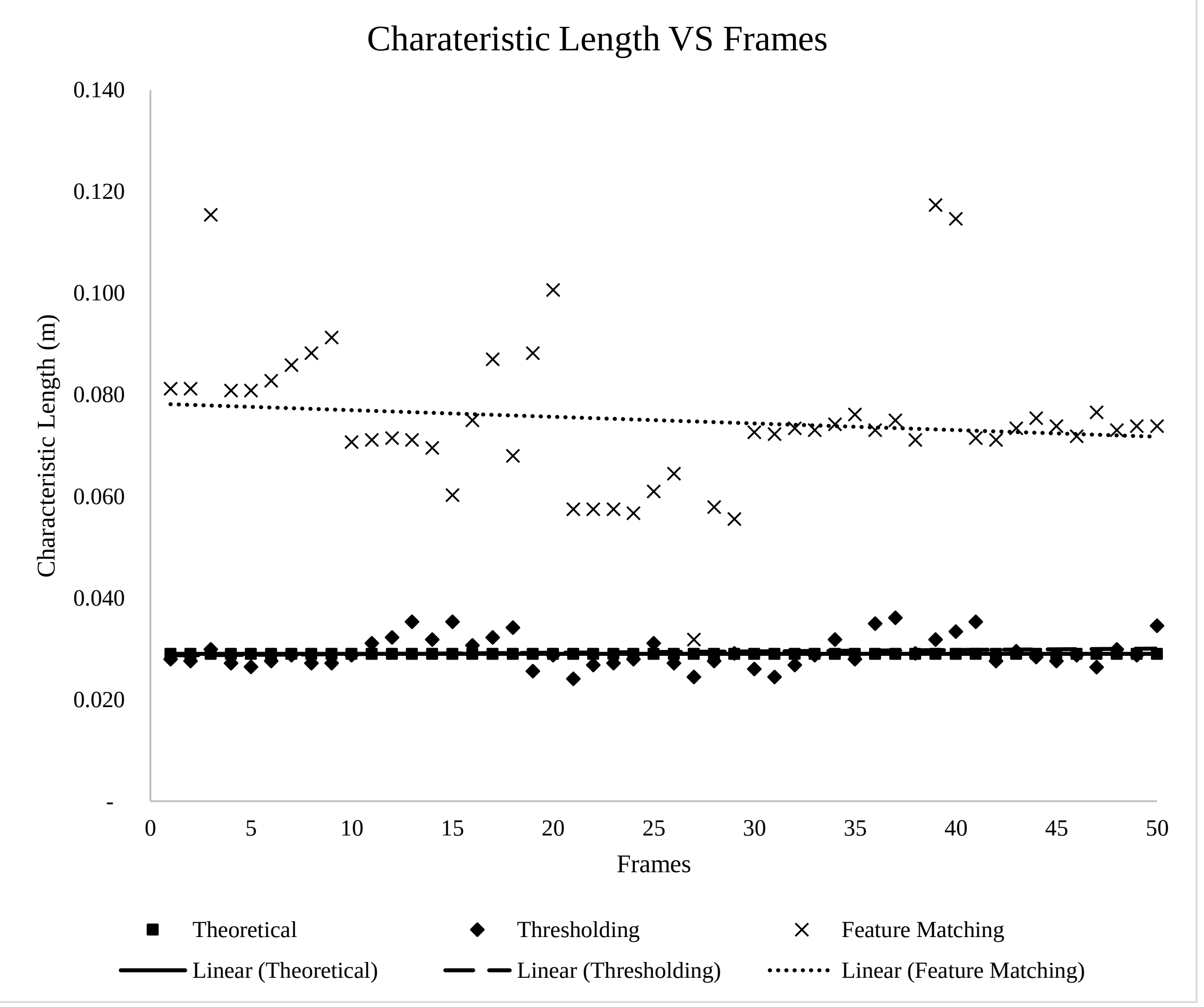

FIGURE 4.5 A table of actual characteristic length versus theoretical characteristic length

Figure 4.5 shows the compilation of the results of image processing techniques obtained over 50 frames of fluid flow video. The theoretical characteristic length is 0.029 m. Out of the three image processing techniques, only thresholding and features tracking are able to yield results. The characteristic length yield from thresholding technique produce result ranging between 0.024 m to 0.036 m. The characteristic length yield from feature matching technique product result ranging between 0.035 m to 0.0115 m. It was suspected that the inconsistency yield in the results might be caused by movement of the flow particles in the image. The fluid flow image moves over time. Hence, the characteristic length detected by the image processing technique fluctuates. The reason for textural filters unable to differentiate the turbulent flow regime may be due to there is no difference in textural properties of a single phase fluid flow.

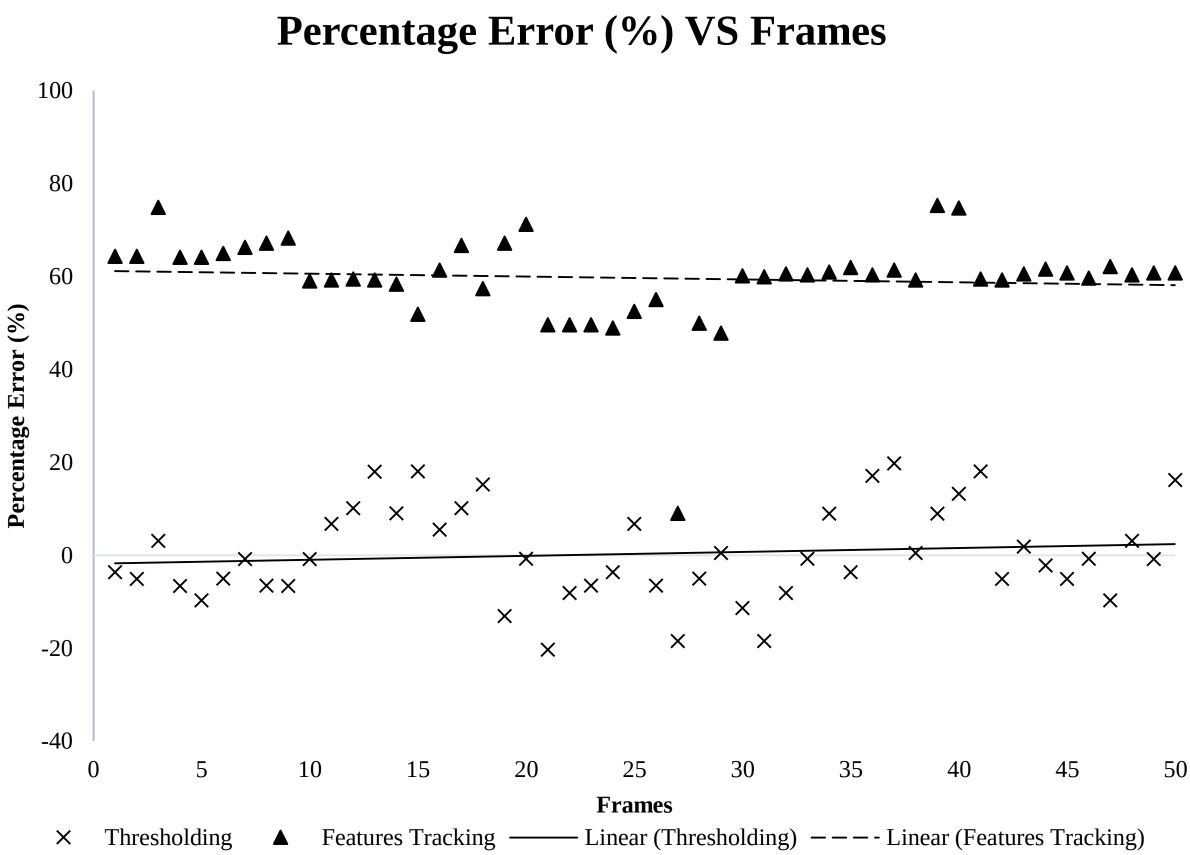

FIGURE 4.6 A table of accuracy of image processing technique versus frames.

Figure 4.6 shows the compilation of accuracy of the image processing technique used versus frames. The result shows that thresholding provides a better turbulent flow regime identification when compared to feature matching technique. Thresholding technique yield a percentage error of approximately 5% and feature matching technique a percentage error of 60%.

For thresholding technique, the error percentage is considered to be low. Despite the acceptable results, it was suspected that the error might be caused by the threshold technique used was not sensitive enough to characterize the flow regimes accurately. Numerous runs using image with contrast enhancement, histogram equalization and noise removal filters does not provide a more accurate result. Hence, it is safe to assume that the source of error shall not be coming from the quality of the image. Other attempts to increase the sensitivity of the threshold value yield little or no changes. Thus, it is safe to say that the error might be coming from the image processing technique itself. In an actual application, it is recommended to provide an equal lighting to the region of interest (ROI) and first perform image enhancement techniques to ensure the image is at its best condition. Then, a more sensitive level of thresholding value will be recommended to use. Instead of varying the threshold value in the increment of +/- of 0.1, the increment should be reduced to the value of +/- 0.01. Varying the threshold value with a smaller increment should provide a more precise result. Besides, the optimum threshold value should be determined after analyzing the histogram of the image. The threshold value should be in between the two peaks of the histogram. Application such as MATLAB image segmentation app with the features of automatic thresholding can be used to determine the optimum threshold level.

For feature matching, the percentage error may be caused by inaccuracy in the training image. The accuracy of the technique depends on the training image. When a training image of the theoretical turbulent flow regime was used, the percentage error of the technique reduced from an average level of 60% to 20%. Figure 4.7 shows the table of the percentage error versus frame on the improvement of results. This shows that the technique relies on the quality of the training image. In addition, the image processing technique may not be able to differentiate precisely between turbulent flow regime and transitional flow regime as both flow regimes have the chaotic properties. Turbulent flow regime has a higher level of chaotic properties.

For textural filters technique, it was unable to yield any results. It was suspected that the problem lies in the image itself. For a single phase flow image, there will be same level of entropy and energy existing throughout the flow. This can be clearly observed when the filters used were changed. Three types of filters were used to try out the applicability of the technique on this project. The filters used were entropy filter, Gabon filter and range filter. The were no clear differentiation between the flow regimes. Hence, it is safe to assume that textural filters technique is not applicable for characterizing single phase turbulent flow.

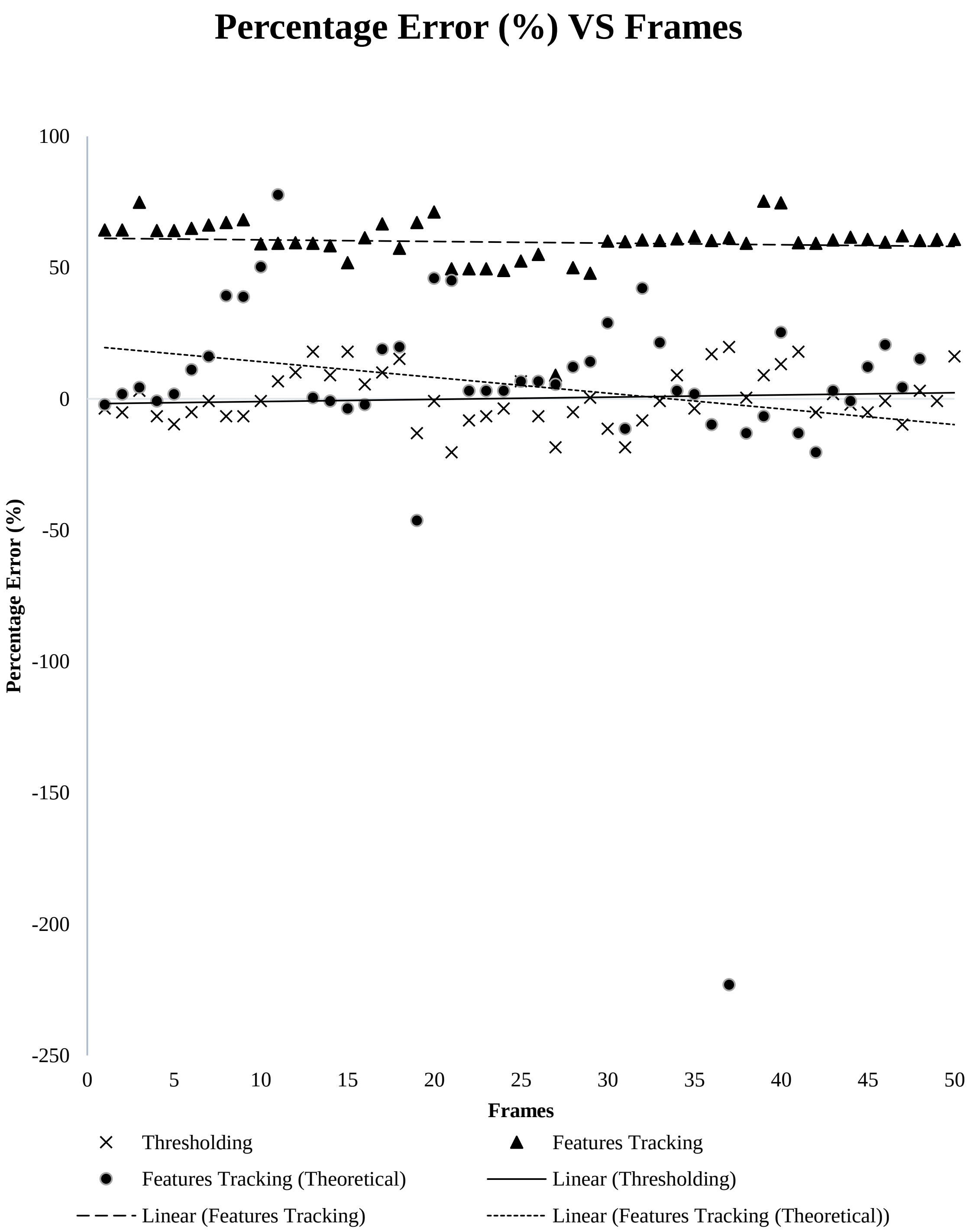

FIGURE 4.6 A table of accuracy of image processing technique versus frames.

CHAPTER 5

CONCLUSION AND RECOMMENDATION

To conclude, as per the results, single phase turbulent flow regimes can be distinguished using basic image processing technique. Out of the three techniques, thresholding, feature tracking and textural filter, only thresholding and feature tracking are able to yield results. Thresholding technique yield the closest result with a percentage error of 5%, feature tracking on the other hand yield a percentage error of 60%. Despite the acceptable results, the reason of causing the percentage error might be due to the limitations of the thresholding technique. For features matching on the other hand, the cause of the high percentage error is due to the inaccuracy of the training image used for feature matching technique. The similar features existing in transitional flow regime and turbulent flow regime may be one of the source of error as well. When an accurate turbulent flow regime training image was used for feature matching technique, the error percentage reduce to 20%. This shows that the accuracy of the training image is the main contributor to the source of error. The accuracy of the techniques can be further improved and validated using various type of flow images. For future work, the relationship between the optical properties of the single phase turbulent flow regime and other single phase flow regime should be studied to improve the accuracy of the techniques. Techniques that are able to classify all three single phase flow regimes (laminar, transitional and turbulent) are recommended to be explored in future. The applicability of this technique to various types of single phase flow can be further studied on too.

References

[1] M. K. McNutt, R. Camilli, T. J. Crone, G. D. Guthrie, P. A. Hsieh, T. B. Ryerson, O. Savas and F. Shaffer, “Review of flow rate estimate of the Deepwater Horizon Oil spill,” In *Proceedings of Natural Academy of Science,* vol. 109, no. 50, pp. 20260-20267, 2012.

[2] Crone T. J. & Tolstoy M., “Magnitude of the 2010 Gulf of Mexico Oil Leak,” *Science*, 330:634, 2010.

[3] Shuib A. S., Hoskins P. R., and Easson W. J., “Flow regime characterization in a diseased artery model,” *International Journal of Medical, Health, Biomedical, Bioengineering and Pharmaceutical Engineering*, vol. 4, no. 2, pp. 51–55, 2010.

[4] Meinhart C. D., Werely S. T., and Santiago J. G., “PIV measurements of a microchannel flow,” *Experiments in fluids*, vol. 27, no. 5, pp. 414–419, 1999.

[5] Durst F., “Turbulent flows,” in *Fluid Mechanics. An introduction to the theory of fluid flow*. Heidelberg, Berlin: Springer-Verlag, pp. 558–559, 2008.

[6] Crone T. J., Mcduff R. E., and Wilcock W. S. D., “Optical plume velocimetry: a new flow measurement technique for use in seafloor hydrothermal systems,” *Exp Fluids*, vol. 45, no. 5, pp. 899-915, 2008.

[7] J. Ebling, G. Scheuermann, “Segmentation of Flow Fields using Pattern Matching” in *Eurographics/ IEEE-VGTC Symposium on Visualization*, Thomas Ertl, Ken Joy, and Beatriz Santos. 2006.

[8] J. Ebling, G. Scheuermann, B. Van Der Wall: “Analysis and Visualization of 3-D PIV Images from HART II Using Image Processing Methods”. In *Data Visualization 2005*, pp. 161–168, 2005.

[9] F. H. Post, B. Vrolijk, H. Hauser, R. S. Laramee, H. Doleisch. “The State of the Art in Flow Visualization: Feature Extraction and Tracking.” *Computer Graphics Forum,* vol. 22, (4), pp: 1-17, 2003.

[10] I. A. Sadarjoen and F. H. Post. “Geometric methods for vortex detection”. In *Data Visualization ’99*. Proc. VisSym’99, pp: 53–62, 1999.

[11] Tobias O. J., "Image segmentation by histogram thresholding using fuzzy sets," IEEE Transactions on Image Processing, vol. 11, no. 12, pp. 1457-1465, 2002.

[12] T. W. Ridler & S. Calvard, "Picture thresholding using an iterative selection method." IEEE Transactions on Pattern Analysis and Machine Intelligence, vol. 10, no. 6, 1988.

[13] J. S. Weszaka, R. N. Nagel & A. Rosenfeld, "A threshold selection technique." IEEE Transactions on Computers, vol. C-23, pp. 1322- 1326, 1974.

[14] N. Otsu, "A threshold selection method from grey- level histogram" IEEE Transactions on Systems, Man and Cybernetics, vol. SMC-9, no. 1, 1979.

[15] K. Samiee & G. A. Rezai Rad, "Textural Segmentation of Side scan Sonar Images Based on Gabor Filters Bank and Active Contours without Edges." In *IEEE Fifth International Conference on Advanced Video and Signal Based Surveillance*, 2008.

[16] A. Sindhuja & V. Sadasivam, "Unsupervised textural segmentation of SonoElastographic breast images" In *International Conference on Sustainable Energy and Intelligent Systems*, Chennai, pp: 744- 748, 2011.

[17] A. Mojsilovic, M. V. Popovic, A. N. Neskovic and A. D. Popovicq, "Wavelet image extension for analysis and classification of infarcted myocardial tissue", In *IEEE transaction on Bio-medicine Engineering*, vol.44, pp: 856-866, 1997.

[18] Shirley Selvan, M. Kavitha, S. Shenbagadevi and S. Suresh, "Feature Extraction for Characterization of Breast Lesions in Ultrasound Echography and Elastography," IN Journal of Computer Science, vol. 6, issue 1, pp: 67-74, 2010.

[19] J. H. Spurk and N. Aksel, "Fundamentals of turbulent flow," in *Fluid Mechanics*, 2nd ed., Heidelberg, Berlin: Springer-Verlag, pp. 205–206, 2008.

[20] B. R. Munson, T. H. Okiishi, W. W. Huebsch, and D. F. Young, "Appendix B Physical Properties of Fluids," in *Fundamentals of Fluid Mechanics*, 6th ed., Wiley & Sons (Asia) Pte. Ltd., 2010